# On-orbit Calibration of ADEOS OCTS with an AVIRIS underflight.

Robert O. Green, Betina Pavri, Joseph W. Boardman, Masanobu Shimada and Hiromi Oaku

NASA Jet Propulsion Laboratory / California Institute of Technology

## 1.0 Introduction

The Ocean Color Temperature Scanner (OCTS) onboard the Advanced Earth Observation Satellite (ADEOS) was launched on August 17, 1996. Calibration of OCTS is required for use of the on-orbit measured data for retrieval of physical properties of the ocean. In the solar reflected portion of the electromagnetic spectrum, OCTS measures images with nominally 700 m spatial resolution through eight multispectral bands (Table 1). The objective of this research was to establish the absolute radiometric calibration of OCTS on-orbit through an underflight by the Airborne Visible/Infrared Imaging Spectrometer (AVIRIS). AVIRIS is a NASA earth-observing imaging spectrometer designed, built and operated by the Jet Propulsion Laboratory (JPL). AVIRIS acquires data from 20 km altitude on a NASA ER-2 aircraft, above most of the Earth's atmosphere. AVIRIS measures the solar reflected spectrum from 370 nm to 2500 nm through 224 contiguous spectral channels. The full width at half maximum (FWHM) of the spectral channels is nominally 10 nm. AVIRIS spectra are acquired as images of 11 km by up to 800 km extent with 20 m spatial resolution. The high spectral resolution of AVIRIS data allows direct convolution to the spectral response functions of the eight multispectral bands of OCTS (Figure 1). The high spatial resolution of AVIRIS data allows for spatial re-sampling of the data to match the ADEOS sensors spatial resolution. In addition, the AVIRIS high spatial resolution allows assessment of the scaling effects due to environmental factors of thin cirrus clouds, sub-pixel cloud cover, white caps, ocean foam, sun-glint, and bright target adjacency. The platform navigation information recorded by AVIRIS allows calculation of the position and observation geometry of each spectrum for match to the OCTS measurement. AVIRIS is rigorously characterized and calibrated in the laboratory prior to and following the flight season (Chrien et al., 1990, 1996). The stability and repeatability of AVIRIS calibration have been validated through an extensive series of inflight calibration experiments (Green et al., 1988,1996, 1998). In the OCTS portion of the spectrum, using pre and post flight runway calibrations of AVIRIS coupled with the on-board calibrator (Green et al. 1993, Chrien et al., 1995) an absolute calibration accuracy of better than 3% spectral (Green, 1995), 2% radiometric (Figure 2) and 5% spatial (Chrien and Green, 1993) has been achieved.

An analogous satellite underflight calibration experiment was performed with AVIRIS and the Optical Sensor (OPS) onboard the Japanese Earth Resources Satellite (JERS) (Green et al. 1993, 1997).

Table 1. OCTS Visible to Near-Infrared Data Characteristics

---

SPECTRAL

| Band | Center | FWHM |
|------|--------|------|
| 1 | 0.412 μm | 20 nm |
| 2 | 0.443 μm | 20 nm |
| 3 | 0.490 μm | 20 nm |
| 4 | 0.520 μm | 20 nm |
| 5 | 0.565 μm | 20 nm |
| 6 | 0.665 μm | 20 nm |
| 7 | 0.765 μm | 40 nm |
| 8 | 0.865 μm | 40 nm |

**RADIOMETRIC**
Digitization          10 bits

**GEOMETRIC**
Field of view          40° (1500km)
Instantaneous FOV      0.85 mrad  (~700 m)

Table 2.  AVIRIS Data Characteristics

**SPECTRAL**
Wavelength range          370 to 2500 nm
Sampling                  10 nm
Spectral response (fwhm)  10 nm
Calibration               <1nm

**RADIOMETRIC**
Radiometric range         0 to maximum Lambertian radiance
Sampling                  ~ 1 DN noise RMS
Absolute calibration      <= 96 %
Calibration Stability     <= 98 %
Polarization Sensitivity  <= 1 %
Noise                     Exceeding NEdL/SNR requirement

**GEOMETRIC**
Field of view             30 degrees (11 km)
Instantaneous FOV         1.0 mrad (20 m)
Calibration               <=0.1 mrad
Flight line length        800 km

## 2.0 Data

On the 20th of May 1997 AVIRIS underflew the ADEOS OCTS sensor of the coast of Southern California near latitude 36.12 and longitude 128.25. The OCTS sensor was tilted to the Northeast to avoid sun glint. In order for the AVIRIS spectral images to overlap the area, the azimuth, and the zenith angles of the OCTS measurements, AVIRIS was flown in a circle (Figure 3) beneath OCTS (Figure 4). The AVIRIS scan angle (+-15 degrees) plus the aircraft roll angle (15 degrees) assured overlap of both area and observation geometry. The data from the 20th of May 1997 flight were spectrally, radiometrically and spatially calibrated through the AVIRIS data system algorithms. The OCTS data were requested as uncalibrated digitized numbers at the sensor. Both the AVIRIS and the OCTS data sets included the position and pointing information at the time of acquisition. The simultaneous acquisition of the AVIRIS and OCTS with overlapping observation geometry provides the essential data set to complete the calibration objective.

## 3.0 Analysis

Determination of the areas of the OCTS and AVIRIS images with the same observation geometries requires projection of the data based on the position and pointing of the sensor. As new set of algorithms were developed to calculate the azimuth (Figure 5) and zenith (Figure 6) angles of the AVIRIS spectra based on the Global Positioning System (GPS) and Inertial Navigation System (INS) information recorded from the ER-2 aircraft. For the geometric calculations, the GPS provided the latitude, longitude and altitude of ER-2 and the INS provided the roll, pitch and yaw of the ER-2 aircraft. The position of AVIRIS is know with respect to the ER-2 aircraft with some uncertainty introduced by the +-1.5 degree AVIRIS automatic roll correction. A related set of algorithms were developed and used to calculate the azimuth (Figure 7) and zenith angles (Figure 8) of the OCTS image. As with AVIRIS, the satellite sensors position and pointing information were supplied with the OCTS image data. With both the AVIRIS and OCTS image azimuth and zenith angles determined, the area of overlap was determined (Figure 9). This area contains the AVIRIS spectra and OCTS band of the same area on the surface with the same observation azimuth and zenith. The average AVIRIS spectrum from this area was extracted (Figure 10). A correction factor was applied for the transmittance from the 20 km AVIRIS altitude to the top of the atmosphere (Figure 11). This transmittance correction factor was calculated with the MODTRAN radiative transfer code (Berk et al., 1989, Anderson et al., 1995). The Ozone was constrained by the amount reported in the TOVS total ozone archive for the area of acquisition (http://nic.fb4.noaa.gov/products/stratosphere/tovsto/archive/np/ ). The corrected AVIRIS spectrum was convolved to the 8 solar reflected OCTS multispectral bands (Figure 12). On-orbit radiometric calibration coefficients for OCTS were calculated as the ratio of the AVIRIS radiance propagated to the top of the atmosphere and the OCTS digitized numbers with dark signal subtracted (Table 3). Uncertainties were trace to the uncertainty in AVIRIS absolute radiometric calibration. The resulting on-orbit OCTS radiometric calibration coefficients were the objective of the AVIRIS underflight of OCTS and this research.

Table 3. ADEOS OCTS AVIRIS Based Radiometric Calibration Coefficients.

| Band | OCTS DN | AVIRIS Radiance* | OCTS RCC** | RCC** Uncertainty |
|------|---------|------------------|------------|-------------------|
| 1 | 2.119E+03 | 7.673E+00 | 3.620E-03 | 1.086E-04 |
| 2 | 2.013E+03 | 7.220E+00 | 3.587E-03 | 7.174E-05 |
| 3 | 1.841E+03 | 5.661E+00 | 3.075E-03 | 5.535E-05 |
| 4 | 1.400E+03 | 4.254E+00 | 3.040E-03 | 4.864E-05 |
| 5 | 1.199E+03 | 2.787E+00 | 2.325E-03 | 3.720E-05 |
| 6 | 9.242E+02 | 1.383E+00 | 1.496E-03 | 2.842E-05 |
| 7 | 7.814E+02 | 7.174E-01 | 9.181E-04 | 1.653E-05 |
| 8 | 1.064E+03 | 5.008E-01 | 4.708E-04 | 8.004E-06 |

* $\mu W/cm^2/nm/sr$
** $\mu W/cm^2/nm/sr/DN$

## 4.0 Conclusion

The eight solar reflected multispectral bands of the OCTS sensor onboard the ADEOS satellite have been calibrated by an underflight of the AVIRIS imaging spectrometer. This calibration was enabled by the AVIRIS characteristics of: high spectral resolution; high spatial resolution; large image extent; accurate spectral, radiometric, and spatial calibration; high altitude flight, and accurate position and pointing knowledge. In addition, a new set of software modules have been developed to project AVIRIS spectra and satellite sensor multispectral data based on platform position and pointing information. These software modules will support future spaceborne sensor calibration efforts with AVIRIS.

This AVIRIS based method is an important independent approach to establish the calibration of spaceborne optical sensors in the solar reflected spectrum. This approach calibrates the spaceborne sensor in the operational on-orbit environment with signal level appropriate to the satellite sensor measurement objectives.

Increasingly rigorous calibration requirements are being established for Earth-looking satellite sensors to support physically based data analysis. Calibration is also required to support measurement and monitoring of the Earth system through time. The calibration of satellite sensors must be established and validated on-orbit where the operational measurement objectives of the sensor are accomplished. The sensor characteristics AVIRIS in conjunction with the rigorous calibration of AVIRIS enables a new strategy for the on-orbit calibration of satellite optical imaging sensors with a range of spatial, spectral, and radiometric resolutions in the solar reflected spectrum.

## 5.0 Acknowledgments

## 6.0 References

Anderson, G. P., Wang, J., Chrtwynd, J. H., (1995), MODTRAN3: An update and recent validation against airborne high resolution inferometer measurements, *Summaries of the Fifth Annual JPL Airborne Earth Science Workshop.*, JPL: Pasadena, California, 5-8

Berk, A., L. S. Bernstein, and D.C. Robertson, MODTRAN: A Moderate Resolution Model for LOWTRAN 7, Final report, GL-TR-0122, AFGL, Hanscomb AFB, MA., 42 pp. 1989.

Chrien, T. G., Green, R. O., Eastwood, M. L. (1990), Accuracy of the spectral and radiometric laboratory calibration of the Airborne Visible/Infrared Imaging Spectrometer, Proceedings of the Second Airborne Visible/Infrared Imaging Spectrometer (AVIRIS) Workshop., JPL: Pasadena, California, 1-14.

Chrien, Thomas G; Green, RO, 1993, Instantaneous Feild of View and Spatial Sampling of the Airborne Visible/Infrared Imaging Spectrometer (AVIRIS), Summaries of the Fourth Annual JPL Airborne Geoscience Workshop, Vol 1. AVIRIS, JPL Pub 93-26

Chrien, Tomas G; Eastwood, M; Green, RO; Sarture, C; Johnson, H; Chovit, C; Hajek, P, 1995, Airborne Visible Infrared/Visible Imaging Spectrometer (AVIRIS) Onboard Calibration System, Summaries of the Fifth Annual JPL Airborne Earth Science Workshop, Vol 1. AVIRIS, JPL Pub 95-1

Chrien, Thomas G; Green, RO; Chovit, CJ; Eastwood, ML; Sarture, CM,1996, Calibration of the Airborne Visible/Infrared Imaging Spectrometer in the Laboratory, Summaries of the Sixth Annual JPL Airborne Earth Science Workshop., JPL: Pasadena, California

Green, R. O., Vane, G. A., Conel, J. L., (1988), Determination of in flight AVIRIS spectral, radiometric, spatial, and signal to noise characteristics using atmospheric and surface measurements from the vicinity of the rare earth bearing carbonatite at Mountain Pass, California, Proceedings of the Airborne Visible/Infrared Imaging Spectrometer (AVIRIS) Performance Evaluation Workshop., JPL: Pasadena, California, 162-184

Green, Robert O 1993, Use of Data from the AVIRIS Onboard Calibrator, Summaries of the Fourth Annual JPL Airborne Geoscience Workshop, Vol 1. AVIRIS, JPL Pub 93-26

Green, Robert O; Conel, JE; van den Bocsh, J; Shimada, M ,1993, Use of the Airborne Visible/Infrared Imaging Spectrometer to Calibrate the Optical Sensor on Board the Japanese Earth Resources Satellite-1, Summaries of the Fourth Annual JPL Airborne Geoscience Workshop, Vol 1. AVIRIS, JPL Pub 93-26

Green, Robert O,1995, Determination of the In-Flight Spectral Calibration of AVIRIS Using Atmospheric Absorption Features, Summaries of the Fifth Annual JPL Airborne Earth Science Workshop, Vol 1. AVIRIS, JPL Pub 95-1

Green, Robert O; Conel, JE; Margolis, J; Chovit, C; Faust, J,1996, In-Flight Calibration and Validation of the Airborne Visible/Infrared Imaging Spectrometer (AVIRIS), Summaries of the Sixth Annual JPL Airborne Earth Science Workshop., JPL: Pasadena, California

## 7.0 Figures

Figure 1. The OCTS bands and AVIRIS spectral channels for the spectral region from 400 to 1000 nm are shown. Also shown is a modeled high resolution radiance spectrum for an ocean target.

Figure 2. AVIRIS radiometric uncertainty based on the transfer of the radiance calibration standard to the AVIRIS sensor.

Figure 3. AVIRIS flight circle under the ADEOS OCTS sensor on the 20th of May 1997.

Figure 4. OCTS image for the 20th of May 1997.

Figure 5. AVIRIS azimuth angles for the calibration data set.

Figure 6. AVIRIS zenith angles for the calibration data set.

Figure 7. OCTS azimuth angles for the calibration data set.

Figure 8. OCTS zenith angles for the calibration data set.

Figure 9. Area of overlap in azimuth and zenith angles between AVIRIS and OCTS for the 20th of May 1997 data set.

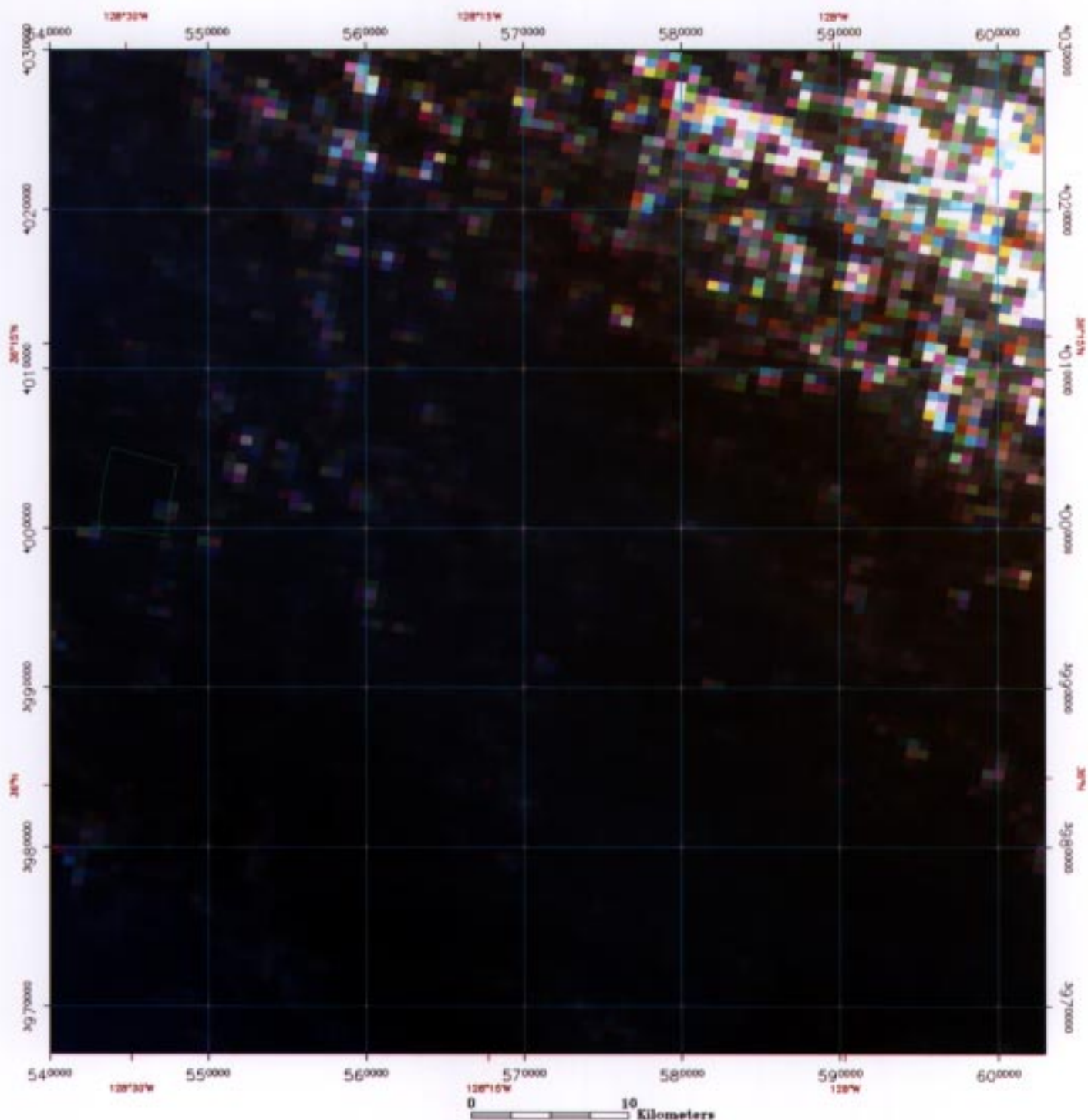Figure 10. AVIRIS spectrum average for the area of geometric overlap between AVIRIS and OCTS .

Figure 11. Transmittance from the AVIRIS altitude of 20 km to the top of the atmosphere.

Figure 12. AVIRIS spectrum average convolved to the spectral response function of OCTS multispectral bands.

AVIRIS Data 970520
matching view geometry shown in green box
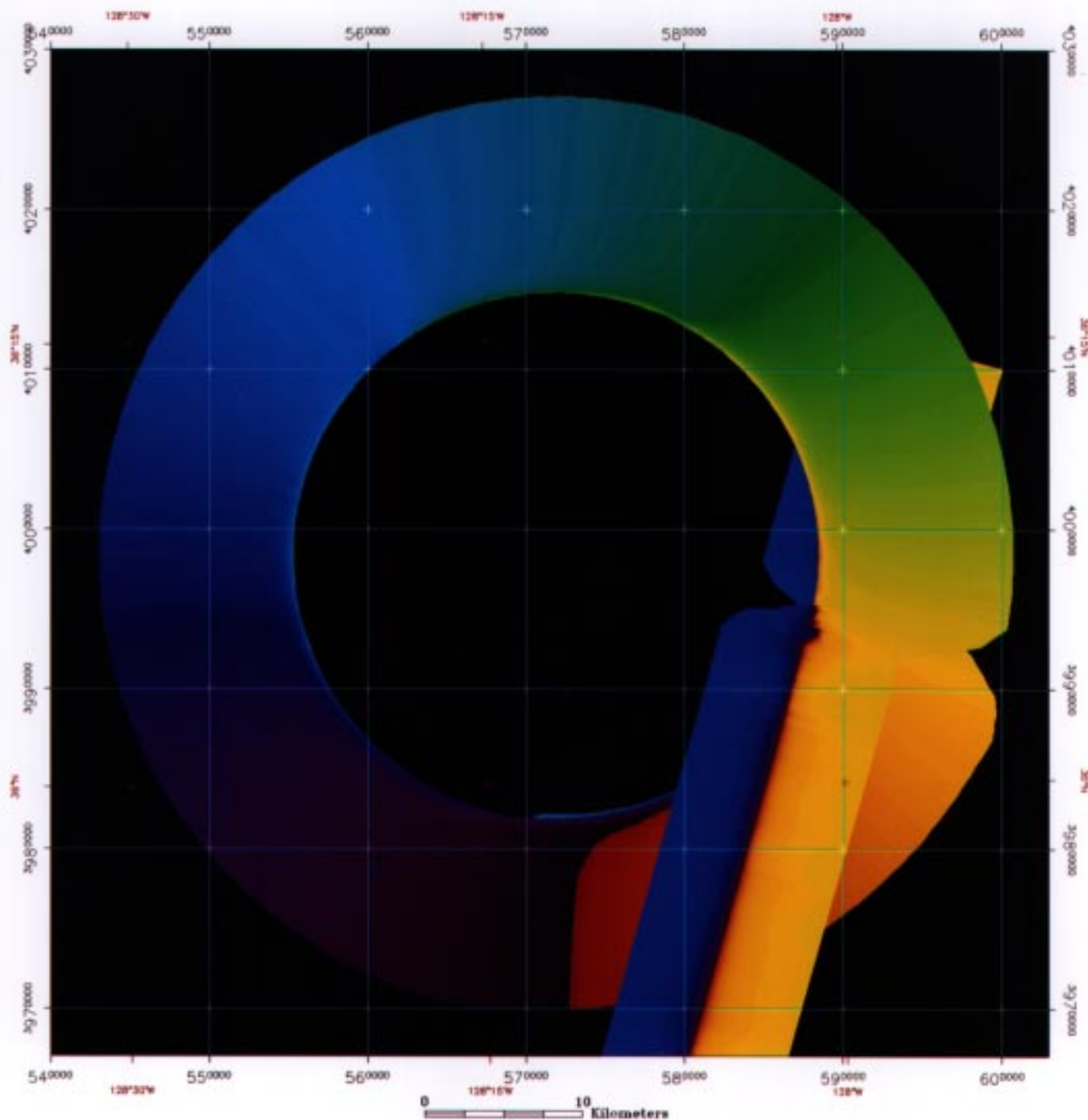UTM zone 9 projection
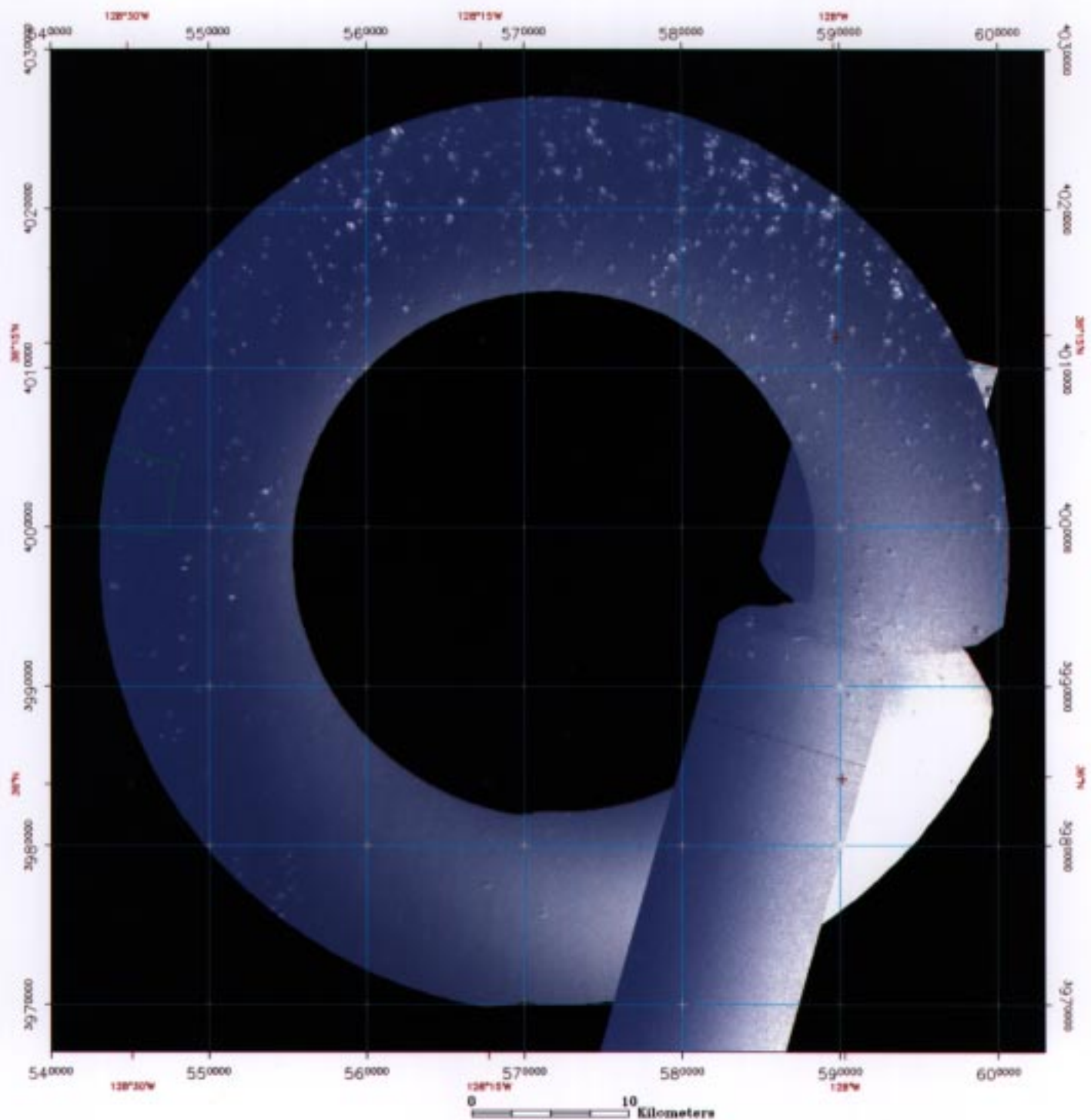
OCTS Data D129000052000218.01
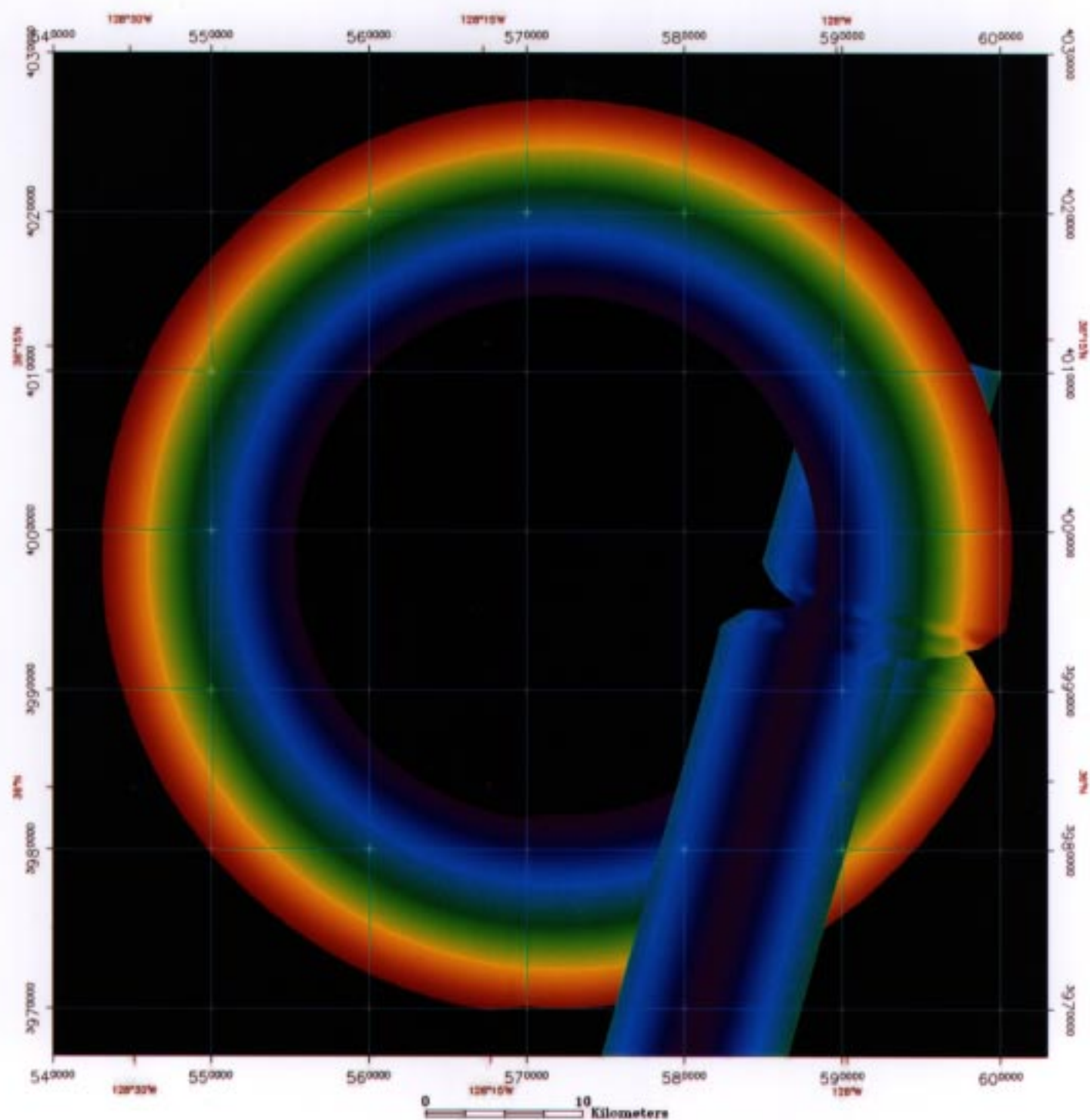matching view geometry shown in green box
UTM zone 9 projection
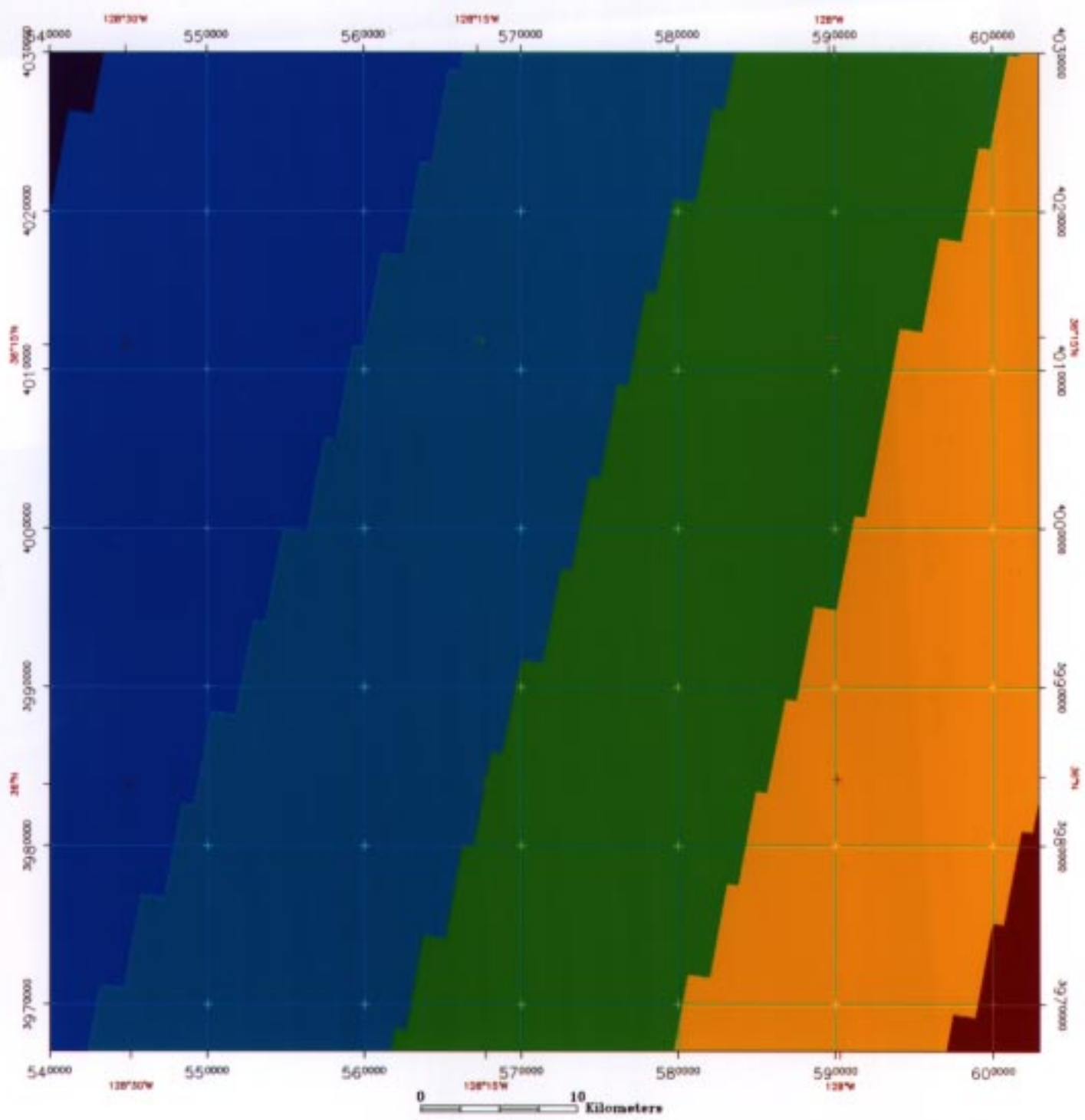
AVIRIS Sensor Azimuth Angle
UTM zone 9 projection

0.0 ███████████ 360.0
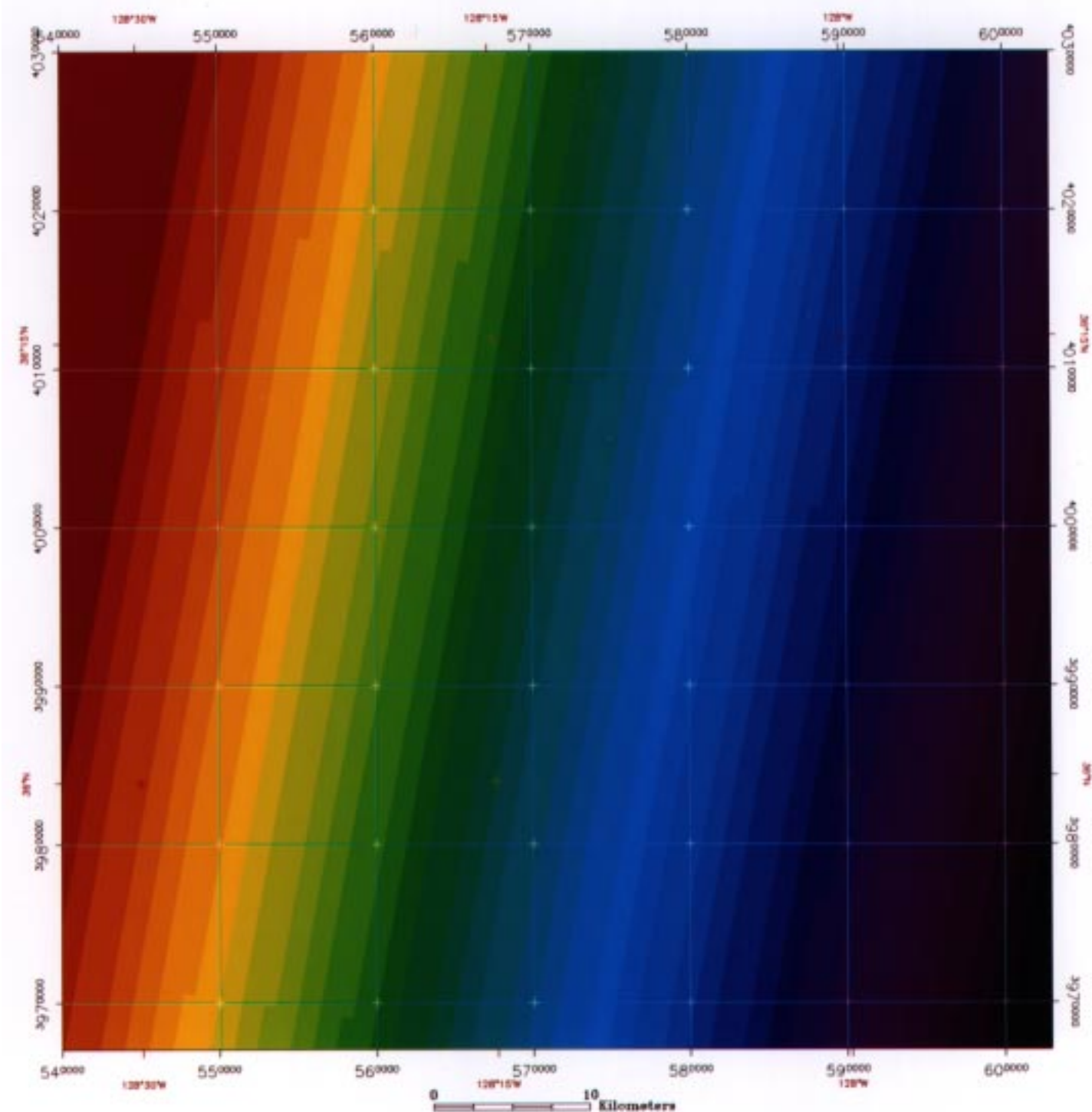
AVIRIS Sensor Zenith Angle
UTM zone 9 projection

0.0 ▬▬▬▬▬▬ 30.1

Figure #7

# OCTS Sensor Azimuth Angle
## UTM zone 9 projection

100.0 ▬▬▬▬▬▬ 100.5

OCTS Sensor Zenith Angle
UTM zone 9 projection

21.9 ▬▬▬▬ 26.2

# AVIRIS/OCTS Matching View Geometry
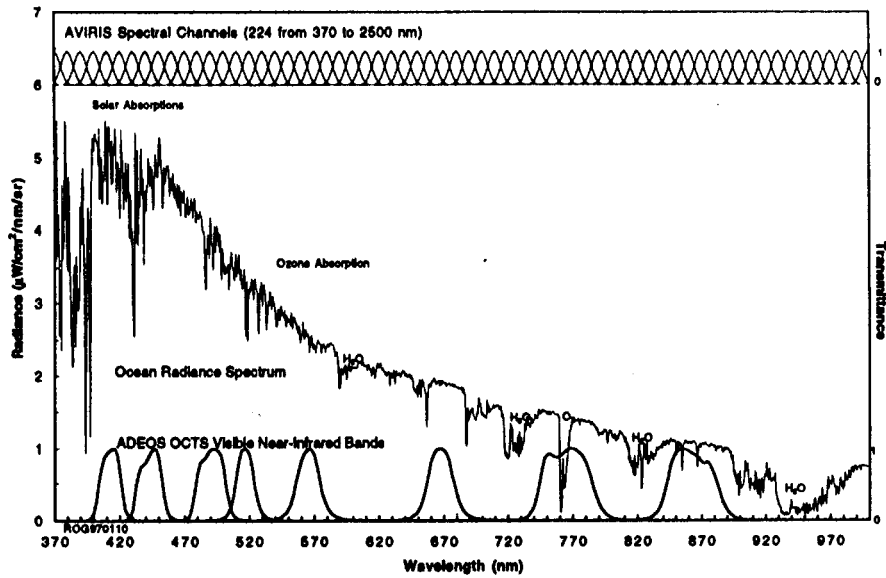## Zenith and Azimuth Within 5 Degrees
## UTM zone 9 projection
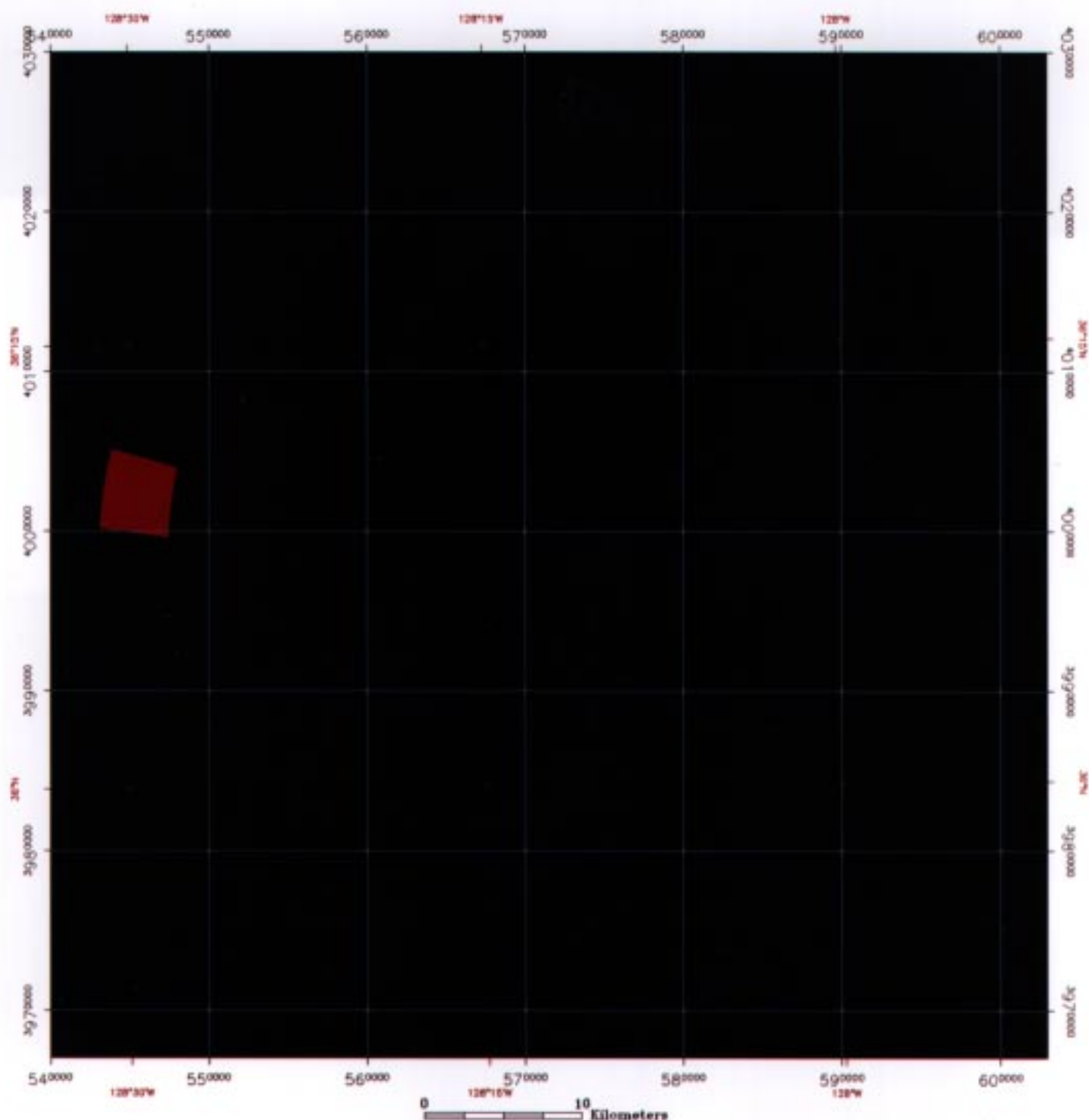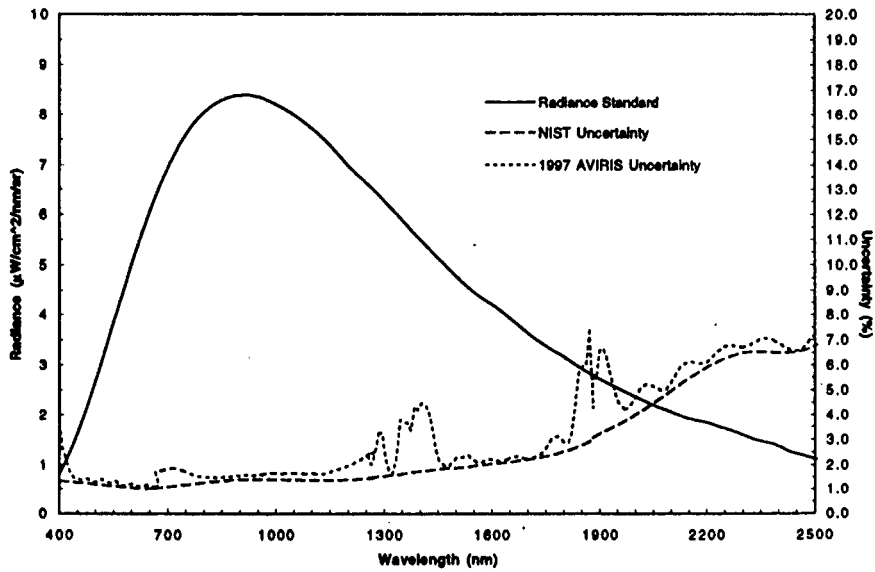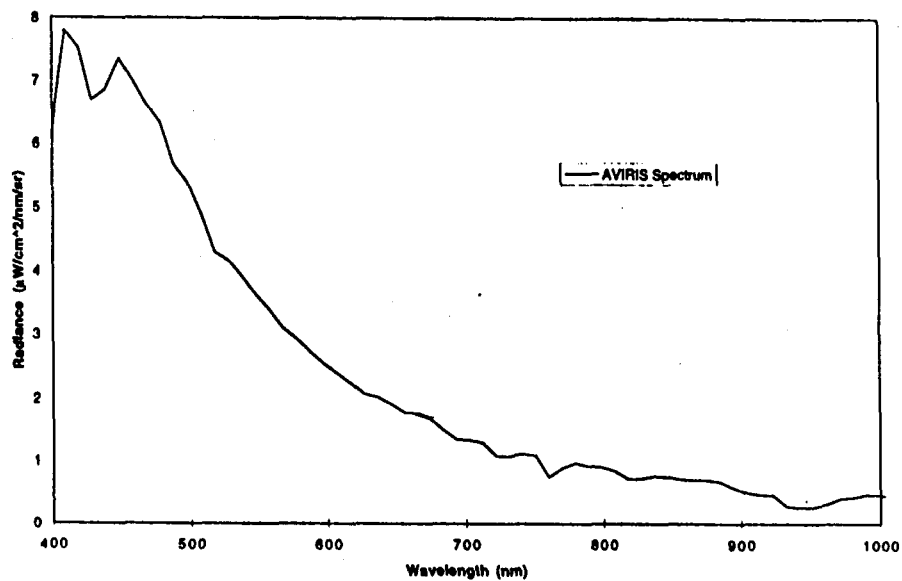
Figure #1



Chart1 (2)

Figure #2

Figure#10

Chart3 (3)



Page 1

Chart1 (2)

Figure #11



Page 1

Chart3 (2)

Figure #12